

Thermal Management of Electric Vehicles Batteries using Phase Change Material

Syed Muneef Ali Shah

USPCAS-E, Thermal Energy Engg
NUST, H-12, Main Campus, Islamabad
muneefshah@gmail.com

Majid Ali

USPCAS-E, Thermal Energy Engg
NUST, H-12, Main Campus, Islamabad
majid@casen.nust.edu.pk

Adeel Javed

USPCAS-E, Thermal Energy Engg
NUST, H-12, Main Campus, Islamabad
adeeljaved@uspcase.nust.edu.pk

Abstract

Due to lower emissions and efficiency of automobile industries are gradually shifting from Internal Combustion (IC) engines to electric motors for vehicle's propulsion. It consists of hybrid and fully electric cars. Hybrid is a combination of both IC engine and electric motors which makes it more efficient and environmental friendly as compared to conventional vehicles. These electric motors are powered by battery packs which contain large number of cells with high energy densities. During acceleration and slope, electric motors pull huge amount of power from battery packs which increases the discharge rates. Higher Discharge rates (C) greatly increase battery's temperature which affects both its life time and performance. To keep battery in optimum temperature, it requires proper thermal management systems. There are some conventional methods for cooling battery packs, but they need extra machinery, cost and space. This paper proposes a passive cooling technique in which Phase Change Material (PCM) is wrapped around battery's cell. Due to high latent heat it can store large amount of heat generated inside battery by keeping its temperature constant. A 3D numerical model of battery and PCM is simulated using ANSYS (Fluent.16). Multi-scale multi-dimensional (MSMD) battery, Solidification/melting and Energy equations are used. Battery cell is discharged at different C-rates without integration of PCM. This process is repeated for battery cell wrapped in PCM. Temperature difference was recorded before and after PCM was attached. Battery cell temperature was lowered by 5 kelvins.

Keywords—Batteries, Thermal management, Temperature, PCM, ANSYS(Fluent)

1. INTRODUCTION

Battery is one of the important components of Electric Vehicle (EV) which costs more than 50% of EV total cost. To lower the maintenance cost, it needs proper

thermal management. High power charging and discharging increases battery's temperature which causes the battery to degenerate at a faster rate. To counter this problem [1] uses four different types of PCM which were wrapped around EV battery, their cooling effects and liquid fraction were compared. For simplicity EV is moving at a constant speed keeping discharge rate constant. Sodium Sulfate Decahydrate is considered the best option due to high latent heat and melting point matching battery requirements. It can maintain battery temperature under 50 Celsius for 2.5 hours.

Al-Zareer et al. [2] used propane as a heat transfer medium to thermally manage Hybrid Electric Vehicle (HEV) battery pack. EV battery is discharged at 4-C without propane movement in the channels. Battery's temperature reached 45 Celsius in 600 secs cycle. Battery is then discharged at the same rate with pumping propane through the channels. This thermal management system-maintained battery's temperature under 35 Celsius. As channels were in contact with battery's cells therefore it kept a uniform temperature on the surface of the cell. Dawood et al. [3] analyzed thermal power of lithium-ion battery through experiment and simulation. 55 Ah lithium-ion battery cell was used for research. Discharging process is the main factor in rising cell's temperature. Most of the heat is generated at the center of cell while air only passes through sides causing nonuniform temperature distribution inside cell. Temperature of cell also increases above 50 Celsius after 2 cycles of charging and discharging. Therefore, Air cooling is not an effective way to keep battery in optimal condition. Z. Ling et al [4] studied the cooling effect on passive thermal management of EV batteries. It concludes that after 2-3 cycles of charging and discharging thermal storage capacity of PCM runs out which leads to failure as temperature of battery pack exceeds 60 Celsius during 1.5-2C discharge. Natural convection

is unable to restore thermal storage of PCM. Air speed is the main factor in the cooling effect of battery. Dincer et al. [5] investigated on maximum temperature of battery's cell integrated with PCM shells of different widths (3mm, 6mm, 12mm). These results were further compared to battery's cell which was discharged at 2-C for every cycle. PCM integration can decrease cell temperature by 5 kelvins. Rao et al.[6] analyzed the effects of thermal conductivity (K_{PCM}) and melting point of PCM wrapped around a $LiFePO_4$ battery which consist of 9 cells. Battery is discharge at 5-C with and without PCM. Battery's temperature without PCM at 5-C discharge rate can reach 60 Celsius easily. After wrapping all battery cells in PCM with melting point of 50 Celsius it can restrict battery maximum temperature under 50 Celsius. Madani et al.[7] gives insight into the discharge behavior of lithium-ion cell. Battery cell is designed using Multi-Scale Multi-Dimension model of fluent (ANSYS). Cell is simulated using three different methods, Newman's Pseudo-2D, NTGK and Equivalent Circuit Model (ECM). This cell is discharge from 0.5C-5C. Effects of discharge rate on cell temperature is studied. Chen et al.[8] does analysis of four different cooling techniques, air cooling, fin cooling, direct and indirect liquid cooling for thermally managing EV battery. Main purpose is to keep battery's cell under 50 Celsius while discharge rates are from 1C-3C. Advantages and disadvantages of all four techniques were compared and indirect liquid cooling has the lowest maximum temperature rise. Only indirect cooling technique can retain battery's cell under ideal conditions and manages an even temperature patterns through the cell.

In all the literature reviews temperature regulation is the key problem in EV batteries. Heat generation mainly occurs during discharging which effect both battery's lifespan and efficiency. In the present work an Aluminum container with 3mm of diameter filled with PCM is integrated to a Toyota Prius battery cell. N-octadecane is used as PCM due to high latent heat and non-corrosivity. Battery's cell is discharged both at lower and higher rates with and without integration of PCM. A clear temperature difference is detected in the results. This thermal management system can sustain cell temperature for serval charge and discharge cycles due to lower heat generation during

charging. Decrease in heat generation also decreases temperature which provides time to PCM to restore some of its heat storing capacity.

2. MATHEMATICAL MODELING

A. Battery model

A lithium-ion cell of 6.5Ah capacity with height of 194 mm, length 146 mm and width 5.4 mm is used for all simulations. Fig. 1 shows picture of battery's cell that is selected for analysis. A 3-dimensional design of cell is built using Design Modular ANSYS (Fluent). It consists of positive tab, negative tab and a cell. Electrodes are made of up Copper while cell is made up of Aluminum. Electrical properties of cell are listed in Table 1.

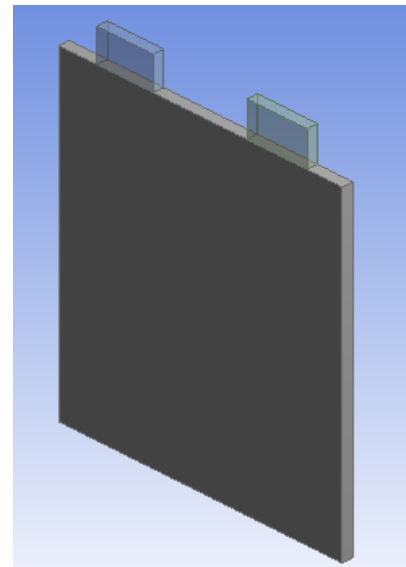


Fig. 1. Cell Geometry

Cell consist of negative material, positive material and separator. Cell model is simulated in fluent using Multi-Scale Multi-Dimensional (MSMD) module. MSMD also contain User Define Functions (UDF) which allow users to design batteries according to its requirements.

Table 1. Electrical Properties of Cell

| Property | Rating | Unit |
|-------------------------|--------|------|
| Nominal Cell Capacity | 6.5 | Ah |
| Specific System Current | 19.5 | A |
| Specific System Voltage | 1.2 | V |
| Specific System Power | 23.4 | W |
| Minimum Stop Voltage | 2.8 | V |
| Maximum Stop Voltage | 4.3 | V |

Source: Toyota Prius Specifications 04 Prius website

Equations 1 and 2 are used to analyze electrochemical and thermal behavior of battery's cell respectively.

$$\begin{cases} \nabla\sigma_+\nabla^2\phi_+ = -J \\ \nabla\sigma_-\nabla^2\phi_- = -J \\ J = \frac{I}{V} \end{cases} \quad (1)$$

Where σ represents electrodes electric conductivities, $\phi_{+,-}$ is phase potential for positive and negative electrodes. J is for Volumetric transfer of current density which can be obtained from current I divided by V (volume) of the model.

$$\left\{ C_p \frac{\partial p}{\partial t} T - \nabla k \nabla^2 T = \dot{q} \right. \quad (2)$$

$$\dot{q} = \nabla\sigma_+\nabla^2\phi_+ - \nabla\sigma_-\nabla^2\phi_- + JU - J(\phi_+ - \phi_-) - JT \frac{dU}{dT}$$

Where C_p is for specific heat, k for thermal conductivity and ρ for density of battery material. \dot{q} is the heat generation during charging and discharging cycles T is temperature and U represents open circuit voltage of the battery. All these values are listed in Table 2.

Table 2. Thermo-physical Properties Cell material

| Property | Value |
|---------------------------------|-------|
| Density (kg/m^3) | 2092 |
| Specific heat (J/kgK) | 871 |
| Thermal conductivity (w/mK) | 202.4 |

B. PCM Modeling

Heat transfer in PCM is calculated using Enthalpy base method. Table 3 contain thermo-physical properties of PCM. Equations used in simulating heat transfer through PCM are.

$$\frac{\rho \partial H}{\partial t} = \nabla k \nabla T \quad (3)$$

$$H = h + \Delta H \quad (4)$$

$$h = \int_{T_0}^T C_p dT \quad (5)$$

$$\Delta H = \rho \gamma \quad (6)$$

$$\beta = \begin{cases} 0, & T < T_m \\ 1, & T \geq T_m \end{cases} \quad (7)$$

ρ represents density of PCM, k is thermal conductivity, H is enthalpy, h is sensible heat, ΔH indicates enthalpy of melted PCM, β is liquid fraction and γ is specific phase change enthalpy of PCM.

Boundary Conditions

$$t=0; \\ T = T_0$$

Initially both PCM and battery at ambient temperature.

Table 3. Thermal properties of PCM (n-octadecane)

| Properties | Solid Phase $T_s > T$ | Mushy Zone $T_s < T < T_L$ | Liquid Phase $T > T_L$ |
|-----------------------------|--------------------------|----------------------------------|------------------------------|
| ρ (kg/m ³) | 814 | 769 | 724 |
| k (w/mK) | 0.358 | 0.255 | 0.152 |
| C_p (J/kgK) | 2150 | 225000 | 2180 |
| μ (kg/ms) | 2.68×10^{-3} | - | - |
| β (1/K) | 0.0033 | - | - |
| L (j/kg) | 225000 | - | - |
| T_s (K) | 301.15 | - | - |
| T_l (K) | 303.15 | - | - |

Equation (8) represents energy conservation between Cell and PCM interface.

$$\frac{-k_c \partial T}{\partial n} = \frac{-K_{PCM} \partial T}{\partial n} \quad (8)$$

While equation (9) represents boundary conditions between PCM and Aluminum container.

$$\frac{-k_{PCM} \partial T}{\partial n} = \frac{-K_{Al} \partial T}{\partial n} \quad (9)$$

Interface between the cell and ambient conditions is given by Equation (10)

$$\frac{-K_{Al} \partial T}{\partial n} = \alpha (T - T_{amb}) \quad (10)$$

Newman P2D Model present in MSMD battery module is used for cell simulations. Although it requires more computing power, but is more accurate

as compare to other models such as Newman P2D Model and NTGK Empirical Model due to their limited capabilities.

3. SOLUTION METHODOLOGY

ANSYS/ Fluent .16 is used to solve mathematical model of the battery using finite volume method. All simulations were run transiently. Fluent Mesh is used for meshing due to the simplicity of the geometry. Heat generation and temperature at different discharge rates with respect to time and its effect on PCM is monitored. Three fluent models Energy, Solidification/Melting and Multi-Scale Multi-Dimensional (MSMD) were used to solve all equations give above. MSMD module is used to design battery's cell. Newman P2D model is used to enter battery specifications given in Table 3. Initial state of charge is kept 1 for discharging and 0 for charging process. Joule and E-Chemical heat source is turned on in MSMD battery model for thermal and electrical behavior analysis of cell. Solidification and Melting model is used to monitor PCM liquid and mass fractions. Energy equation is for the heat transfer through the whole geometry according to the given boundary conditions. Aluminum container of width 3 mm is place around the cell shown in Fig. 2.

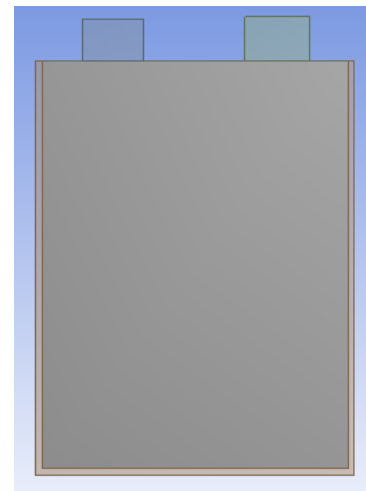


Fig. 2. Battery with PCM

Organic PCM (n-octadecane) is placed inside container. It is non-corrosive, environmental friendly and melting point matches ambient conditions. Heat transfer occurs through all the surfaces where heat

transfer coefficient is $\alpha = 7 \text{ W/m}^2\text{K}$ and $T_{amb} = 301 \text{ K}$. Cell is discharged at 1-C, 2-C and 3-C show in Fig. 3.

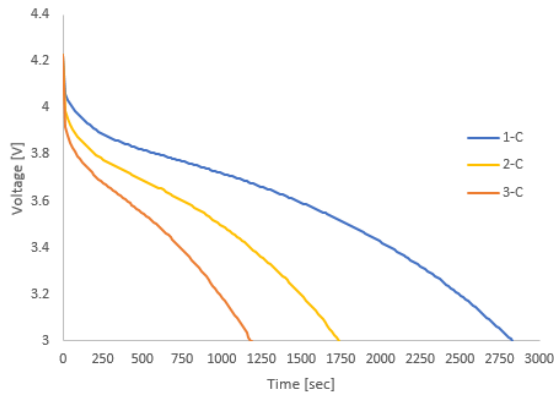


Fig. 3. Discharge curves

4. GRID INDEPENDENCE TEST

Grid independence test is performed to ensure that mesh size does not affect simulations outcome. A property such as temperature is monitored inside the domain to investigate the convergence history. In this paper temperature monitoring is done along X-axis. Three different meshes are consider by changing cell size from 1 to 1.5 and 2 mm. Results of cell size verses temperature are plotted as shown in Fig.4.

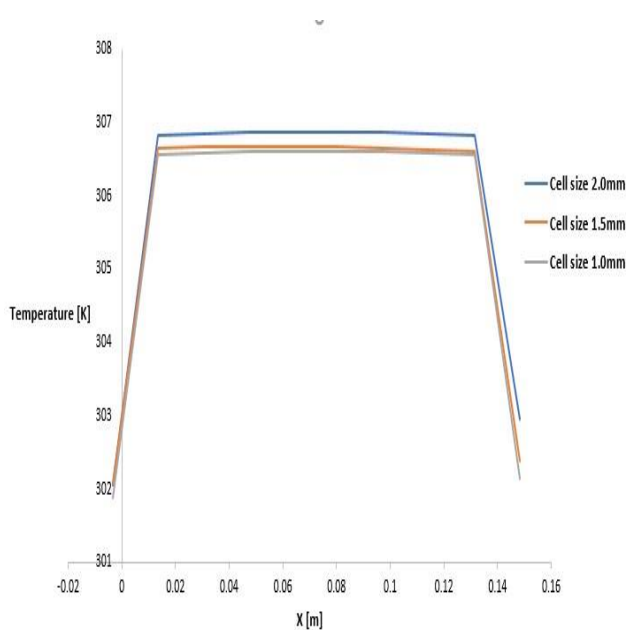


Fig. 4

Changing cell size also changes number of elements as shown in Table 4.

Table 4

| Cell Size (mm) | Number of elements |
|----------------|--------------------|
| 2.0 | 23532 |
| 1.5 | 56152 |
| 1.0 | 186930 |

As shown in Fig. 4 results up to 1.5 mm cell size are constant further increasing cell size decreases number of elements and divergence is started to occur. Therefore, rest of the simulation were run keeping cell size 1.5 mm. Accuracy can increase by 1 mm cell size, but it greatly increases number of elements thus requires greater computing power.

Time step independence test is also carried out to confirm that given time step has no effect on the simulation results. Fig. 5 shows effect on temperature by changing time step.

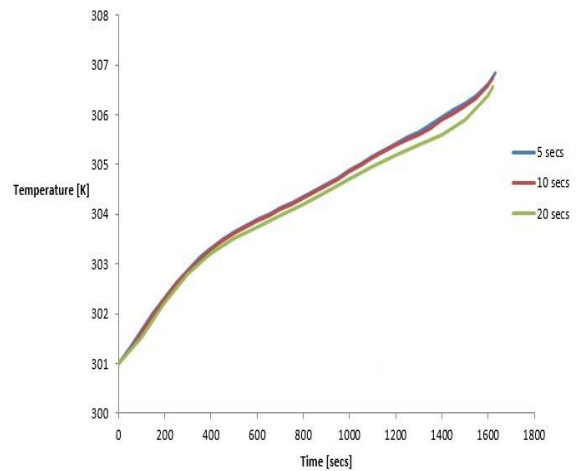


Fig. 5

As shown in Fig. 5 up to 10 sec time step results remain constant on further increasing the time step results start to diverge. For all simulations 1 sec time

step is selected and results is saved after every 15 iterations.

For verification of MSMD battery model results are compared to that of obtained by Dincer et al. [5]. Fig 6 shows comparison of the results. Average temperature difference is constant for different ambient conditions which a good agreement for the validation of further simulations. Therefore, same model is integrated with PCM for further analysis.

5. RESULTS AND DISCUSSION

In this section temperature distribution, maximum temperature, heat generation and discharge at different rates are discussed. Battery cell is discharge at 1.5-C, 2-C, 3-C and 4-C. EV moving in normal conditions is represented by 1 and 2-C, while 3-C is for mild conditions and 4-C represents extreme conditions like hiking a slope. All simulations were run on two geometries of cell. First is without PCM and second one is integrated with PCM. Results of simulation are both compared through contours and graphs. Contours of temperature both with and without PCM are shown in Table 5.

All these contours are results of 2-C discharge which shows temperature distribution inside battery Cell after 300, 600, 1200 and 1600 secs. Maximum temperature can be noted at the bottom of the cell which concludes that most of the heat is generated at this part. It also shows that temperature distribution inside battery cell is non-uniform. Fig. 6 shows maximum temperature difference due to integration of PCM.

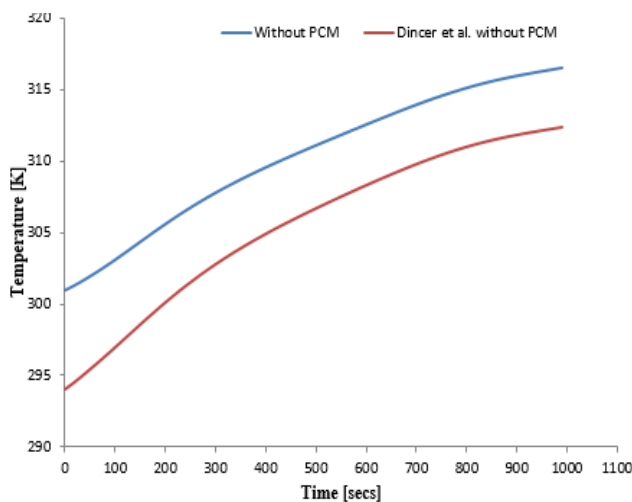


Fig. 6. Transient comparison of average temperature

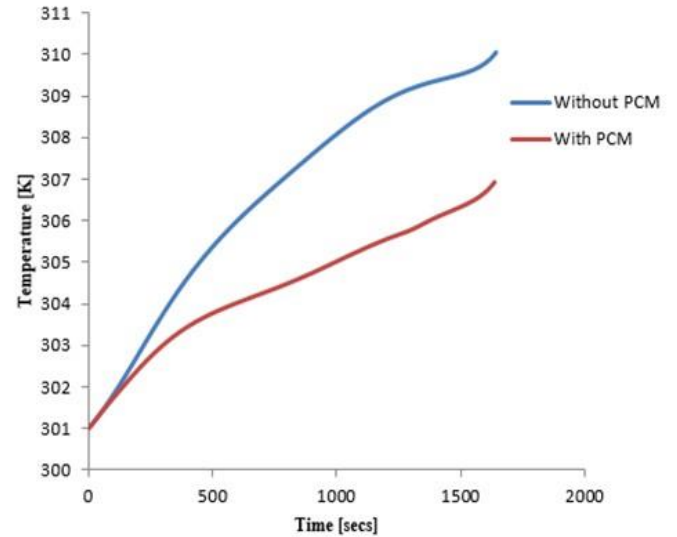


Fig. 7. Maximum temperature difference at 2-C

A difference of 3.5 K is detected after PCM is attach to the cell. It produces a power of 4.45 W and a constant heat of $63,970 \text{ W/m}^3$. As discharges rate of cell increases it also increase heat generation power and temperature. Next Fig. 7 shows maximum temperature difference when discharge rate is 1.5-C, where EV is moving with constant speed without any acceleration. In this case battery will take longer time to discharge and EV will be able to cover longer distance.

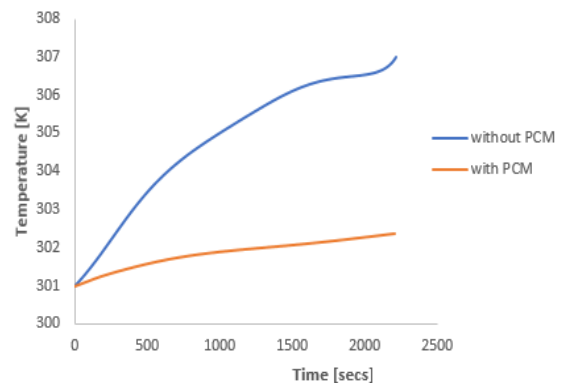


Fig. 8. Maximum temperature difference at 1.5-C

Fig. 8 shows contour of liquid fraction of PCM. As PCM starts to melt its thermal conductivity decreases. In solid state which was 0.358 (w/mK) now decreases to 0.152 (w/mK) which is almost half of it. Fig. 8 shows PCM mass liquid fraction inside container across x-axis.

Table 5. Temperature contours with and without PCM

| Time, secs | No PCM | With PCM |
|------------|--------|----------|
| 300 | | |
| 600 | | |
| 1200 | | |
| 1600 | | |

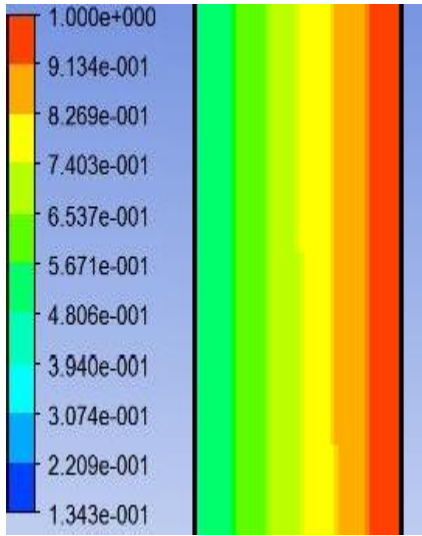


Fig. 9. PCM liquid fraction contour inside container

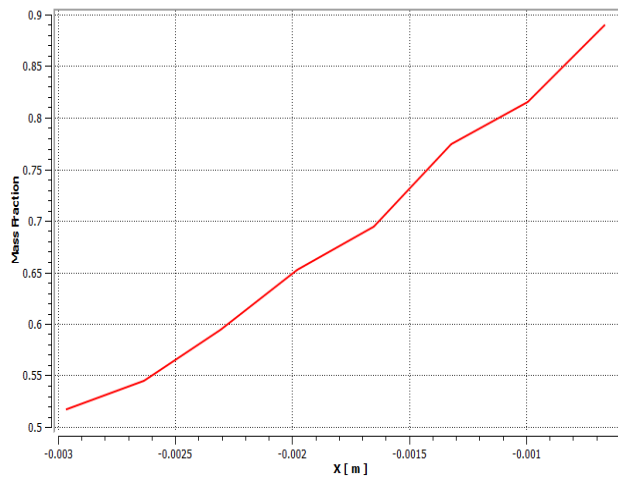


Fig. 10. PCM mass fraction

Maximum temperature due to 3-C and 4-C discharge rates are shown in Fig. 9 and Fig. 10 respectively. As C-rates increases heat generation also increases and so is temperature. At 4-C heat generation reaches 20,000 (w/mK) which is almost double of 2-C. At this point either EV is either accelerating or climbing a slope therefore extract more power form the batteries. Difference between maximum temperatures at higher discharge rates also increases which reaches up to 5 K. Maximum temperature that battery reached at 4-C is 44 Celsius which is still favorable for lithium ion battery. After discharging EV will stop to recharge and battery's temperature will start to decrease

providing enough time for PCM to restore its thermal capacity.

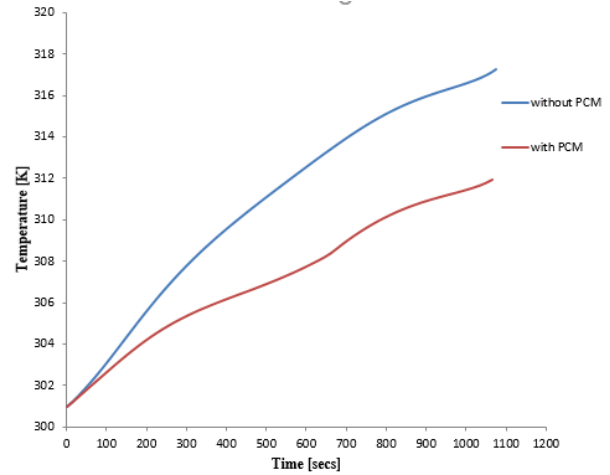


Fig. 11. Maximum temperature difference at 3-C

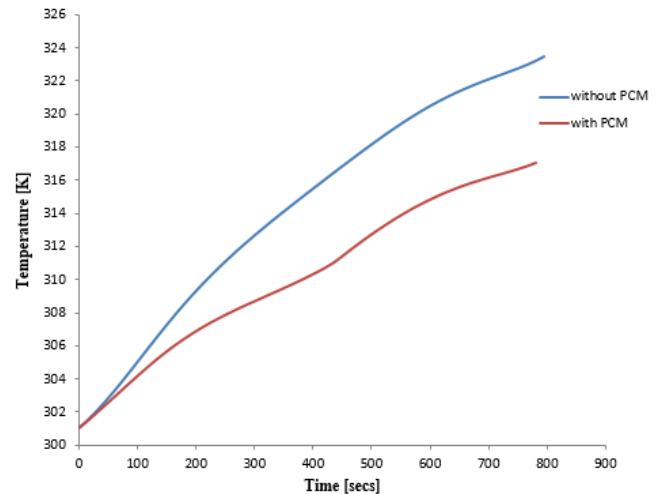


Fig. 12. Maximum temperature difference at 4-C

6. CONCLUSION

PCMs can control the battery temperature effectively. It is found that the width of the container can be reduced to lower the cost as PCM is not completely melted. After the PCM is melted it will have to dissipate the heat to become solid again otherwise it won't be able to absorb more heat therefore it will require a proper convection to have an effective heat transfer from the battery. Increasing further diameter of container up to 12 mm will only lower the

maximum temperature by 0.5 K which is not reasonable due to increase in the cost, weight of battery and extra space requirement.

7. NOMENCLATURE

Capital

| | |
|-------|----------------------|
| C | Discharge rates |
| J | Current density |
| I | Current |
| V | Volume |
| U | Open circuit voltage |
| T | Temperature |
| C_p | Specific heat |
| A | Ampere |
| V | Volt |
| W | Watts |
| H | Enthalpy |
| K | Kelvin |

Small

| | |
|-----------|----------------------|
| \dot{q} | Heat generation |
| k | Thermal conductivity |
| h | sensible heat |
| t | Time |

Greek

| | |
|-------------|--------------------------------|
| σ | electric conductivity |
| \emptyset | Phase potential |
| ρ | Density |
| Δ | Change |
| β | liquid fraction |
| γ | Specific phase change enthalpy |

Subscripts

| | |
|-------|-------------------|
| p | Pressure |
| 0 | initial Condition |
| amb | Ambient |
| Al | Aluminium |
| C | Cell |

Abbreviations

| | |
|------|-------------------------------|
| IC | Internal Combustion |
| C | Discharge rates |
| PCM | Phase Change Material |
| MSMD | Multi-scale multi-dimensional |
| UDF | User Define Functions |

8. REFERENCES

- [1] M. Y. Ramandi, I. Dincer, and G. F. Naterer, "Heat transfer and thermal management of electric vehicle batteries with phase change materials," *Heat Mass Transf.*, vol. 47, no. 7, pp. 777–788, 2011.
- [2] M. Al-Zareer, I. Dincer, and M. A. Rosen, "A novel phase change based cooling system for prismatic lithium ion batteries," *Int. J. Refrig.*, vol. 86, pp. 203–217, 2018.
- [3] B. Dawoud, E. Amer, and D. Gross, "Experimental investigation of an adsorptive thermal energy storage," *Int. J. energy Res.*, vol. 31, no. August 2007, pp. 135–147, 2007.
- [4] Z. Ling, F. Wang, X. Fang, X. Gao, and Z. Zhang, "A hybrid thermal management system for lithium ion batteries combining phase change materials with forced-air cooling," *Appl. Energy*, vol. 148, no. June, pp. 403–409, 2015.
- [5] I. Dincer, H. S. Hamut, and N. Javani, *Thermal Management of Electric Vehicle Battery Systems*. 2017.
- [6] Z. Rao, S. Wang, and G. Zhang, "Simulation

- and experiment of thermal energy management with phase change material for ageing LiFePO₄power battery,” *Energy Convers. Manag.*, vol. 52, no. 12, pp. 3408–3414, 2011.
- [7] S. S. Madani, M. J. Swierczynski, and S. K. Kaer, “The discharge behavior of lithium-ion batteries using the Dual-Potential Multi-Scale Multi-Dimensional (MSMD) Battery Model,” *2017 12th Int. Conf. Ecol. Veh. Renew. Energies, EVER 2017*, 2017.
- [8] D. Chen, J. Jiang, G. H. Kim, C. Yang, and A. Pesaran, “Comparison of different cooling methods for lithium ion battery cells,” *Appl. Therm. Eng.*, vol. 94, pp. 846–854, 2016.